The WiggleZ Dark Energy Survey: joint measurements of the expansion and growth history at $z < 1$

Chris Blake,[1]* Sarah Brough,[2] Matthew Colless,[2] Carlos Contreras,[1] Warrick Couch,[1] Scott Croom,[3] Darren Croton,[1] Tamara M. Davis,[4] Michael J. Drinkwater,[4] Karl Forster,[5] David Gilbank,[6] Mike Gladders,[7] Karl Glazebrook,[1] Ben Jelliffe,[3] Russell J. Jurek,[8] I-hui Li,[1] Barry Madore,[9] D. Christopher Martin,[5] Kevin Pimbblet,[10] Gregory B. Poole,[1] Michael Pracy,[3] Rob Sharp,[2,11] Emily Wisnioski,[1] David Woods,[12] Ted K. Wyder[5] and H. K. C. Yee[13]

[1]*Centre for Astrophysics and Supercomputing, Swinburne University of Technology, PO Box 218, Hawthorn, VIC 3122, Australia*
[2]*Australian Astronomical Observatory, PO Box 296, Epping, NSW 1710, Australia*
[3]*Sydney Institute for Astronomy, School of Physics, University of Sydney, NSW 2006, Australia*
[4]*School of Mathematics and Physics, University of Queensland, Brisbane, QLD 4072, Australia*
[5]*California Institute of Technology, MC 278-17, 1200 East California Boulevard, Pasadena, CA 91125, USA*
[6]*South African Astronomical Observatory, PO Box 9, Observatory 7935, South Africa*
[7]*Department of Astronomy and Astrophysics, University of Chicago, 5640 South Ellis Avenue, Chicago, IL 60637, USA*
[8]*Australia Telescope National Facility, CSIRO, Epping, NSW 1710, Australia*
[9]*Observatories of the Carnegie Institute of Washington, 813 Santa Barbara St., Pasadena, CA 91101, USA*
[10]*School of Physics, Monash University, Clayton, VIC 3800, Australia*
[11]*Research School of Astronomy and Astrophysics, Australian National University, Weston Creek, ACT 2611, Australia*
[12]*Department of Physics and Astronomy, University of British Columbia, 6224 Agricultural Road, Vancouver, BC V6T 1Z1, Canada*
[13]*Department of Astronomy and Astrophysics, University of Toronto, 50 St. George Street, Toronto, ON M5S 3H4, Canada*

ABSTRACT

We perform a joint determination of the distance–redshift relation and cosmic expansion rate at redshifts $z = 0.44$, 0.6 and 0.73 by combining measurements of the baryon acoustic peak and Alcock–Paczynski distortion from galaxy clustering in the WiggleZ Dark Energy Survey, using a large ensemble of mock catalogues to calculate the covariance between the measurements. We find that $D_A(z) = (1205 \pm 114, 1380 \pm 95, 1534 \pm 107)$ Mpc and $H(z) = (82.6 \pm 7.8, 87.9 \pm 6.1, 97.3 \pm 7.0)$ km s^{-1} Mpc^{-1} at these three redshifts. Further combining our results with other baryon acoustic oscillation and distant supernovae data sets, we use a Monte Carlo Markov Chain technique to determine the evolution of the Hubble parameter $H(z)$ as a stepwise function in nine redshift bins of width $\Delta z = 0.1$, also marginalizing over the spatial curvature. Our measurements of $H(z)$, which have precision better than 7 per cent in most redshift bins, are consistent with the expansion history predicted by a cosmological constant dark energy model, in which the expansion rate accelerates at redshift $z < 0.7$.

Key words: surveys – distance scale – large-scale structure of Universe.

1 INTRODUCTION

One of the fundamental goals of observational cosmology is to determine the expansion rate of the Universe as a function of redshift. Measurements of the expansion history, which can be described by the evolution of the Hubble parameter $H(z) = (1 + z) \, \mathrm{d}a/\mathrm{d}t$ with redshift z, where $a(t)$ is the cosmic scale factor at time t, provide one of the most important observational tests of the cosmological models which characterize the different components of the Universe and their evolution with time. In particular, a paramount problem in cosmology is to understand the physical significance of the 'dark energy' which appears to dominate the cosmic energy density today, as described by the phenomenology of the standard cosmological constant cold dark matter (ΛCDM) model.

A number of powerful tools to measure the cosmic expansion history beyond the local Universe have been developed in recent decades. Foremost amongst these probes is the use of distant

*E-mail: cblake@astro.swin.edu.au

Type Ia supernovae (SNe) as standard candles (e.g. Riess et al. 1998; Perlmutter et al. 1999; Amanullah et al. 2010; Conley et al. 2011; Suzuki et al. 2012). The apparent peak magnitude of these supernovae, following certain corrections based on the light-curve shape which decrease the observed scatter in the peak brightness, yield a relative luminosity distance as a function of redshift, i.e. $D_L(z)H_0/c$, where $D_L(z)$ is the luminosity distance, H_0 is the local Hubble parameter and c is the speed of light.

Although such measurements accurately trace the shape of the distance–redshift 'Hubble diagram' in the redshift range $z < 1$, a number of qualifications must be mentioned. First, the expansion history $H(z)$ is not directly measured by supernovae but must be determined as a derivative of the noisy luminosity distances (Wang & Tegmark 2005; Sollerman et al. 2009; Shafieloo & Clarkson 2010). Secondly, obtaining the expansion rate from the luminosity distance requires an additional assumption about spatial curvature, which influences the geodesics followed by photons. Thirdly, despite the impressive and thorough treatment in recent supernovae analyses of the systematic errors which could bias cosmological fits, these systematics now limit the utility of these data sets.

Large galaxy surveys offer a complementary route for mapping cosmic distances and expansion, using two principal techniques. First, the large-scale clustering pattern of galaxies contains the signature of baryon acoustic oscillations (BAOs), a preferred length scale imprinted in the distribution of photons and baryons by the propagation of sound waves in the relativistic plasma of the early Universe. This length scale, the sound horizon at the baryon drag epoch $r_s(z_d)$, may be accurately calibrated by observations of the cosmic microwave background (CMB) radiation and applied as a cosmological standard ruler (Blake & Glazebrook 2003; Seo & Eisenstein 2003). Some applications to galaxy data sets are presented by Eisenstein et al. (2005), Percival et al. (2010), Beutler et al. (2011), Blake et al. (2011b), Padmanabhan et al. (2012) and Anderson et al. (2012).

Given a sufficiently large galaxy survey at a redshift z, the preferred scale may be detected in both the tangential direction on the sky as an enhancement in the number of galaxy pairs with a given angular separation $\Delta\theta$, and in the radial direction as an excess of pairs with redshift separation Δz. If these two signals can be simultaneously extracted by measuring galaxy clustering in tangential and radial bins, they respectively carry information about the angular diameter distance $D_A(z) = D_L(z)/(1 + z)^2$ and the Hubble expansion rate at the survey redshift in units of the standard ruler, $r_s(z_d)/[(1 + z)D_A(z)] \sim \Delta\theta$ and $r_s(z_d)H(z) \sim c\Delta z$. If the galaxy survey only permits the baryon acoustic peak to be detected in the angle-averaged galaxy clustering pattern, then an effective 'dilation scale' distance is measured which consists of two parts $D_A(z)$ and one part $1/H(z)$: $D_V(z) = [(1 + z)^2 D_A(z)^2 cz/H(z)]^{1/3}$ (Eisenstein et al. 2005; Padmanabhan & White 2008).

The second technique through which large-scale structure surveys permit measurement of geometrical distances is the 'Alcock–Paczynski (AP) test' (Alcock & Paczynski 1979). The AP test probes the cosmological model by comparing the observed tangential and radial dimensions of objects which are assumed to be isotropic in the correct choice of model. It can be applied to the two-point statistics of galaxy clustering if redshift-space distortions, the principal additional source of anisotropy, can be successfully modelled (Ballinger, Peacock & Heavens 1996; Matsubara & Suto 1996; Simpson & Peacock 2010). By equating radial and tangential physical scales, independently of any underlying standard ruler, the observable $\Delta z/\Delta\theta \sim (1 + z)D_A(z)H(z)/c$ may be determined (Outram et al. 2004; Marinoni & Buzzi 2010; Blake et al. 2011c).

Therefore, using a combination of BAO and/or AP measurements, large-scale galaxy surveys can supply independent measurements of the distance-redshift relation $D_A(z)$ and expansion history $H(z)$. We note that the Hubble expansion rate as a function of redshift may also be inferred from the relative ages of passively evolving galaxies (Jimenez & Loeb 2002; Carson & Nichol 2010; Stern et al. 2010; Moresco et al. 2012). This is a promising technique albeit subject to assumptions about the stellar populations of these galaxies, in particular about galaxy metallicity at high redshift.

We focus here on distance measurements using the WiggleZ Dark Energy Survey (Drinkwater et al. 2010), which was designed to extend the study of large-scale structure over large cosmic volumes to redshifts $z > 0.5$. The study presented here builds upon two existing distance-scale measurements using the WiggleZ data set: Blake et al. (2011b) reported the measurement of the angle-averaged baryon acoustic peak at redshifts $z = (0.44, 0.6, 0.73)$, and Blake et al. (2011c) applied the AP test to the 2D clustering power spectrum. In this latter study we combined the AP fits with SNe data to estimate the Hubble parameter relative to its local value, $H(z)/H_0$. We here extend these analyses by combining the WiggleZ measurements of D_A^2/H and $D_A H$, including a calculation of the covariance of the statistics, to extract measurements of $D_A(z)$ and $H(z)$ as a function of redshift, in absolute units independent of the value of H_0, based solely on WiggleZ Survey data (and a sound-horizon calibration). Furthermore, by combining these measurements with SNe and other galaxy data sets, we constrain the cosmic expansion rate $H(z)$ as a stepwise function in the redshift range $z < 0.9$, and fit a variety of cosmological models to the results.

2 DATA

2.1 WiggleZ Survey clustering measurements

The WiggleZ Dark Energy Survey (Drinkwater et al. 2010) is a large-scale redshift survey of bright emission-line galaxies which was carried out at the Anglo-Australian Telescope between 2006 August and 2011 January. The galaxy sample utilized by this study is drawn from the final set of observations covering about 800 deg^2 of sky in six regions, including a total of $N = 158\,741$ galaxies in the redshift range $0.2 < z < 1.0$, and is the same data set as used for the analysis of the baryon acoustic peak by Blake et al. (2011b). Our study is based on measurements of the angle-averaged galaxy correlation function and 2D galaxy power spectrum in tangential and radial Fourier bins in three overlapping redshift ranges $0.2 < z < 0.6$, $0.4 < z < 0.8$ and $0.6 < z < 1.0$. The effective redshifts of the measurements in these three redshift slices are $z_{eff} = (0.44, 0.6, 0.73)$ (Blake et al. 2011b). We use overlapping, wide redshift ranges in order to ensure a detection of the baryon acoustic peak in each redshift slice (following Percival et al. 2010) and to provide the best mapping of the distance–redshift relation. We account for the correlations between the measurements when fitting models.

2.2 Fitting the baryon acoustic peak

Blake et al. (2011b) presented our analysis of the WiggleZ galaxy correlation function to map the baryon acoustic peak in these three redshift ranges. The correlation functions contain evidence for the baryon acoustic peak in each redshift slice. Our model for fitting the correlation function measurements to determine the standard-ruler distance is described in section 3.1 of Blake et al. (2011b). Our results are most cleanly expressed as a measurement of the acoustic

Table 1. Results of cosmological model fits to the galaxy correlation functions and power spectra measured in three overlapping redshift slices of the WiggleZ Dark Energy Survey. The acoustic scale parameter $A(z)$ is obtained from the fit to the baryon acoustic peak in the correlation function (marginalizing over the matter density $\Omega_m h^2$, the damping parameter σ_v and the galaxy bias factor) and the parameters $F(z)$ and $f\sigma_8(z)$ are measured using the 2D power spectra (marginalizing over a galaxy bias which is not assumed to be identical to its value in the correlation function fit). The angular diameter distance $D_A(z)$ and Hubble expansion rate $H(z)$ are derived from the measurements of $A(z)$ and $F(z)$ assuming a CMB-motivated prior in $\Omega_m h^2$ in order to calibrate the standard ruler.

Redshift slice	$0.2 < z < 0.6$	$0.4 < z < 0.8$	$0.6 < z < 1.0$
Effective redshift z	0.44	0.60	0.73
$A(z) \equiv 100 D_V(z)\sqrt{\Omega_m h^2}/cz$	0.474 ± 0.034	0.442 ± 0.020	0.424 ± 0.021
$F(z) \equiv (1+z)D_A(z)H(z)/c$	0.482 ± 0.049	0.650 ± 0.053	0.865 ± 0.073
$f\sigma_8(z)$	0.413 ± 0.080	0.390 ± 0.063	0.437 ± 0.072
$D_A(z)$ (Mpc)	1204.9 ± 113.6	1380.1 ± 94.8	1533.7 ± 106.8
$H(z)$ (km s^{-1} Mpc^{-1})	82.6 ± 7.8	87.9 ± 6.1	97.3 ± 7.0

parameter,

$$A(z) = \frac{100 \, D_V(z)\sqrt{\Omega_m h^2}}{c \, z}, \tag{1}$$

at the effective redshift of the sample. We marginalized over the shape of the clustering pattern (parametrized by the physical matter density $\Omega_m h^2$), non-linear damping of the acoustic peak and galaxy bias. The results for $A(z)$ are listed in Table 1, reproduced from Blake et al. (2011b).

2.3 Fitting the 2D power spectrum

Blake et al. (2011c) presented an analysis of the 2D WiggleZ galaxy power spectrum, where modes are binned by Fourier wavenumber and angle to the line-of-sight. We repeated these measurements for the new choice of redshift bins consistent with the correlation function analysis. Our model for fitting the 2D power spectrum to extract the AP distortion is described in section 3.2 of Blake et al. (2011c). At each redshift we obtain a measurement of the distortion parameter $F(z) = (1+z)D_A(z)H(z)/c$ and the normalized growth rate $f\sigma_8$, which quantifies the amplitude of redshift-space distortions in terms of the growth rate f and amplitude of matter fluctuations σ_8. We also marginalized over a linear bias factor which we do not require to be identical to the bias in the correlation function model. This is a conservative choice which reflects the possibility that the amplitude of these two statistics due to galaxy bias and redshift-space distortions may be scale dependent. Fig. 1 displays the joint

likelihoods of F and $f\sigma_8$ fitted in each of the new redshift slices. We note that although there is a strong correlation between the parameters, both may be successfully determined, and the results are collected in Table 1.

3 JOINT FITS FOR THE EXPANSION AND GROWTH HISTORY

3.1 Covariances between fitted parameters

Given that our measurements of the baryon acoustic scale and tangential/radial clustering anisotropy have taken place in overlapping redshift slices, using clustering statistics which are potentially correlated by common cosmic variance, it is important to determine the covariances between the measurements of $(A, F, f\sigma_8)$ within and between redshift slices. This is achieved by repeating the different parameter fits for each of a series of lognormal realizations, and using the statistical ensemble to determine the various correlation coefficients. We generated 400 lognormal realizations for each WiggleZ Survey region and redshift slice (i.e. 2400 realizations for each redshift slice, or 7200 in total) using the methods described by Blake et al. (2011a). Lognormal realizations provide a reasonably accurate galaxy clustering model for the linear and quasi-linear scales which are important for modelling the large-scale clustering pattern.

Fig. 2 displays the correlations between single parameters fit to different pairs of redshift slices. In each panel, the small dots
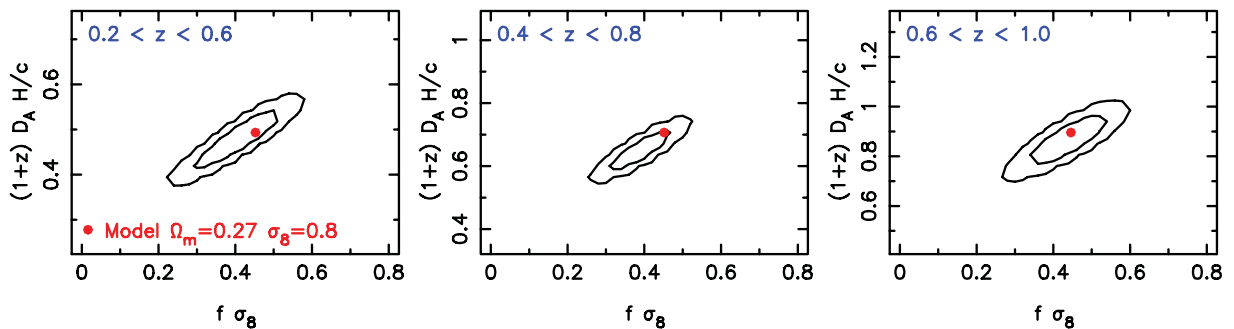

Figure 1. The joint likelihood of the AP scale distortion parameter $F(z) \equiv (1+z)D_A(z)H(z)/c$ and the normalized growth rate quantified by $f\sigma_8(z)$, obtained from fits to the 2D galaxy power spectra of the WiggleZ Dark Energy Survey in three overlapping redshift slices $0.2 < z < 0.6$, $0.4 < z < 0.8$ and $0.6 < z < 1.0$. This figure was produced by marginalizing over the linear bias factor b^2. The probability density is plotted as contours enclosing 68.27 and 95.45 per cent of the total likelihood. The solid circles indicate the parameter values in a fiducial flat ΛCDM cosmological model with parameters $\Omega_m = 0.27$, $\sigma_8 = 0.8$.
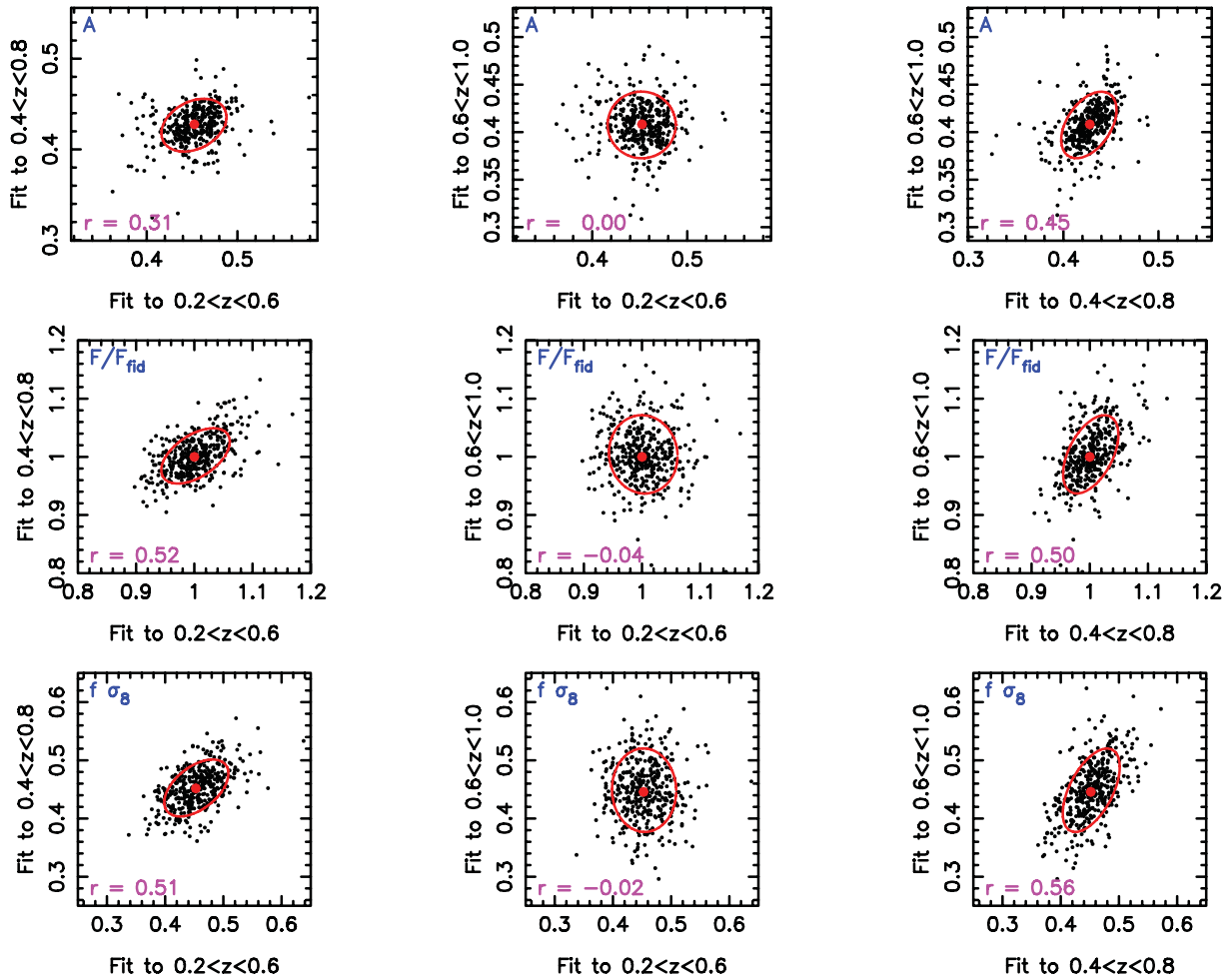
Figure 2. Correlations of the parameters $A(z)$, $F(z)$ and $f\sigma_8(z)$ when each parameter is fitted to pairs of the three overlapping WiggleZ redshift slices. The AP distortion parameter F is plotted relative to its value in the fiducial cosmology, F_{fid}. Each small dot represents the best-fitting values of the parameters using the correlation functions and power spectra measured from 400 independent lognormal realizations. The red ellipses represent the derived covariances between the parameter fits, and the solid red circle is the input fiducial model of the lognormal realizations. The correlation coefficient r is quoted in the bottom left-hand corner of each panel, and is consistent with zero in the second column when non-overlapping redshift slices are used.

represent the best-fitting pairs of parameter values in the redshift slices for the 400 lognormal realizations. The red ellipses are 2D Gaussians representing the covariance between the fitted parameters, and the solid red circle is the input fiducial model used to generate the lognormal realizations. The correlation coefficient r is quoted in the bottom left-hand corner of each panel, and is consistent with zero in the second column when non-overlapping redshift slices are used.

Fig. 3 shows the correlations between pairs of different parameters fit in the same redshift slice, using the same presentation format as Fig. 2. The strongest covariance is measured between the AP distortion F and growth rate $f\sigma_8$ from redshift-space distortions, with correlation coefficients $r \sim 0.8$. The measurements of the baryon acoustic peak 'monopole' parameter A are correlated with each of the 'quadrupole' parameters $(F, f\sigma_8)$ at a lower level $r \sim 0.2$. The full 9×9 covariance matrix for the parameters is listed in Table 2.

Fig. 4 plots the 1D distributions of best-fitting parameters for the second redshift slice, demonstrating that this is well described by the multivariate Gaussian model and does not contain significant wings that might cause the confidence regions to be underestimated in subsequent cosmological parameter fits. The distributions for the other redshift slices are similar.

3.2 Determination of $D_A(z)$ and $H(z)$

Using the joint measurements of the AP distortion parameter $F \propto D_A H$ and acoustic parameter $A \propto (D_A^2/H)^{1/3}$ in each redshift slice, we can break the degeneracy between the angular-diameter distance $D_A(z)$ and Hubble parameter $H(z)$. We fit for D_A and H in each redshift slice using these measurements and their covariance. We also marginalize over the physical matter density $\Omega_m h^2$, which appears in equation (1) for $A(z)$, using a Gaussian prior with mean 0.1345 and width 0.0055. This prior is motivated by fits to the CMB (Komatsu et al. 2009) and is independent of the low-redshift expansion history under certain general assumptions, which are listed in section 5.4.1 of Komatsu et al. (2009).

The joint likelihood of $D_A(z)$ and $H(z)$ in each of the three redshift slices is displayed in Fig. 5, where the solid line represents the joint variation of these parameters with redshift in a fiducial cosmological model $\Omega_m = 0.27$ and $h = 0.71$, and the solid circles superimposed on the line indicate the model prediction for the three analysed redshift slices. The marginalized values of D_A and H at redshifts $z = (0.44, 0.60, 0.73)$ are $D_A(z) = (1205 \pm 114, 1380 \pm 95, 1534 \pm 107)$ Mpc and $H(z) = (82.6 \pm 7.8, 87.9 \pm 6.1, 97.3 \pm 7.0)$ km s^{-1} Mpc^{-1}. A steady increase in the value of
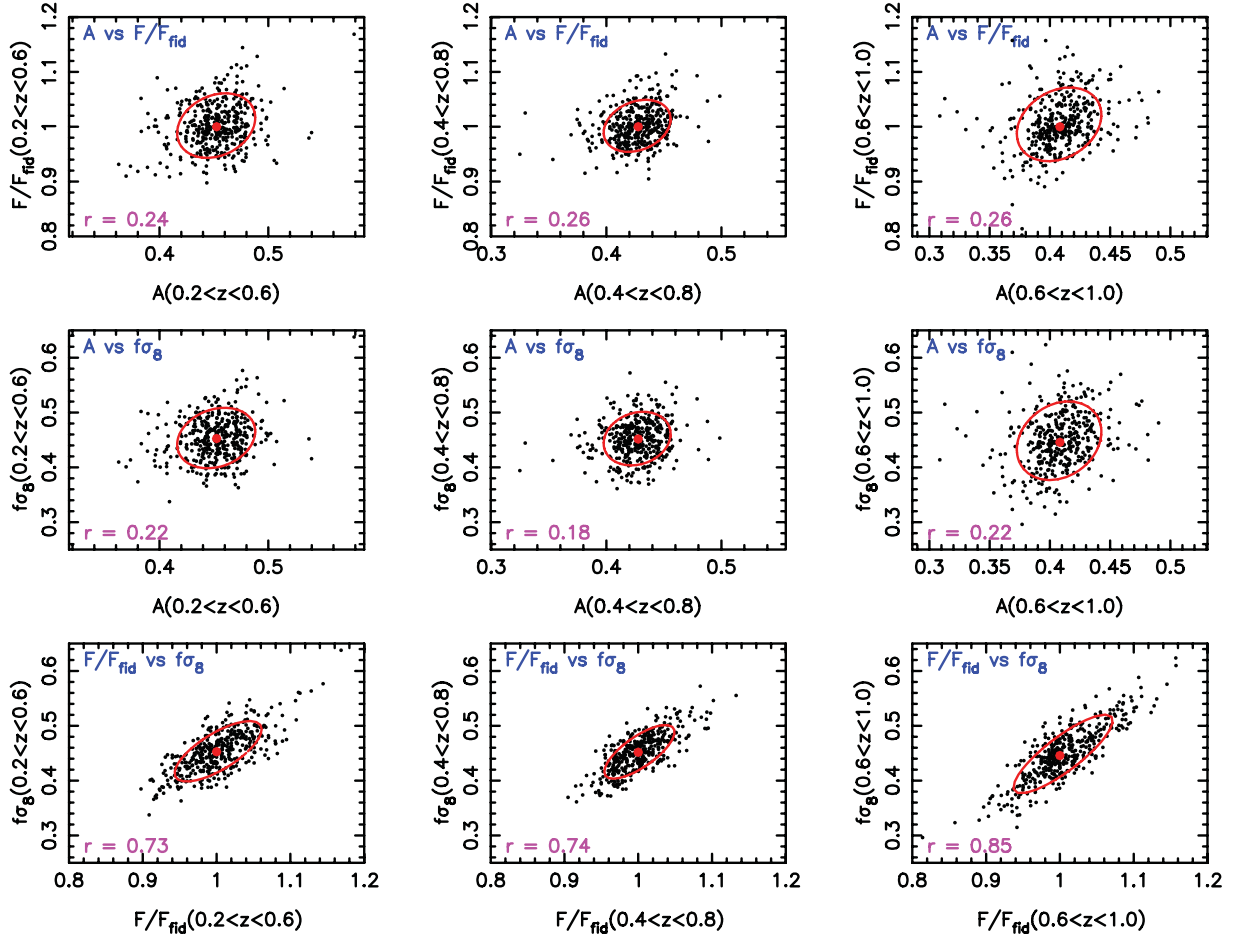
Figure 3. Correlations between different pairs of the parameters $A(z)$, $F(z)$ and $f\sigma_8(z)$ fitted to the three WiggleZ redshift slices. The AP distortion parameter F is plotted relative to its value in the fiducial cosmology, $F_{\rm fid}$. Each small dot represents the best-fitting values of the parameters using the correlation functions and power spectra measured from 400 independent lognormal realizations. The red ellipses represent the derived covariances between the measurements, and the solid red circle is the input fiducial model of the lognormal realizations. The correlation coefficient r is quoted in the bottom left-hand corner of each panel. Although the strongest correlation is obtained between $F(z)$ and $f\sigma_8(z)$, weaker but non-zero correlations are measured between both of these parameters and $A(z)$.

Table 2. This table lists the values of $10^3\underline{\underline{C}}$, where $\underline{\underline{C}}$ is the covariance matrix of measurements from the WiggleZ Survey data of the acoustic parameter $A(z)$, the AP distortion parameter $F(z)$ and normalized growth rate $f\sigma_8(z)$, where each parameter is measured in three overlapping redshift slices (z_1, z_2, z_3) with effective redshifts $z_{\rm eff} = 0.44$, 0.6 and 0.73, respectively, where $z_1 = [0.2, 0.6]$, $z_2 = [0.4, 0.8]$ and $z_3 = [0.6, 1.0]$. The data vector is ordered such that $\underline{Y}_{\rm obs} = (A_1, A_2, A_3, F_1, F_2, F_3, f\sigma_{8,1}, f\sigma_{8,2}, f\sigma_{8,3}) = (0.474, 0.442, 0.424, 0.482, 0.650, 0.865, 0.413, 0.390, 0.437)$. The chi-squared statistic for any cosmological model vector $\underline{Y}_{\rm mod}$ can be obtained via the matrix multiplication $\chi^2 = (\underline{Y}_{\rm obs} - \underline{Y}_{\rm mod})^{\rm T}\underline{\underline{C}}^{-1}(\underline{Y}_{\rm obs} - \underline{Y}_{\rm mod})$. The matrix is symmetric; we just quote the upper diagonal.

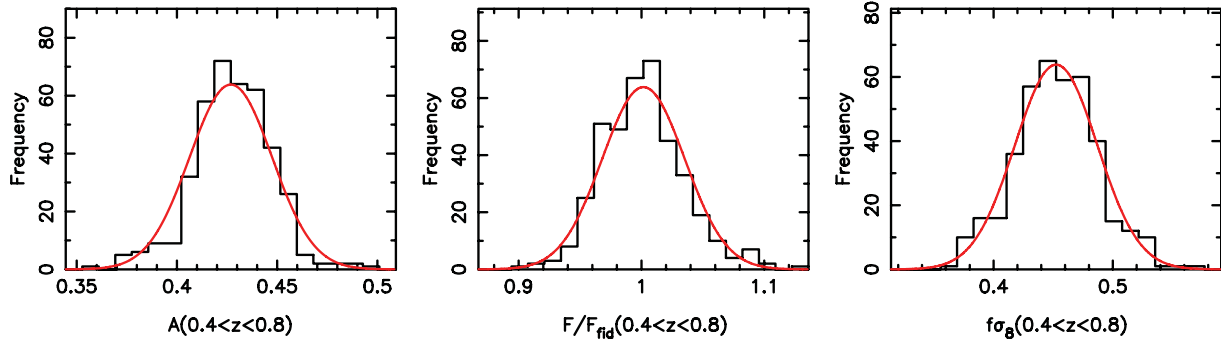| Parameter	$A(z_1)$	$A(z_2)$	$A(z_3)$	$F(z_1)$	$F(z_2)$	$F(z_3)$	$f\sigma_8(z_1)$	$f\sigma_8(z_2)$	$f\sigma_8(z_3)$
$A(z_1)$	1.156	0.211	0.000	0.400	0.234	0.000	0.598	0.129	0.000
$A(z_2)$	–	0.400	0.189	0.118	0.276	0.336	0.080	0.227	0.230
$A(z_3)$	–	–	0.441	0.000	0.167	0.399	0.000	0.146	0.333
$F(z_1)$	–	–	–	2.401	1.350	0.000	2.862	1.080	0.000
$F(z_2)$	–	–	–	–	2.809	1.934	1.611	2.471	1.641
$F(z_3)$	–	–	–	–	–	5.329	0.000	1.978	4.468
$f\sigma_8(z_1)$	–	–	–	–	–	–	6.400	2.570	0.000
$f\sigma_8(z_2)$	–	–	–	–	–	–	–	3.969	2.540
$f\sigma_8(z_3)$	–	–	–	–	–	–	–	–	5.184

Figure 4. The 1D distribution of the best-fitting parameters for 400 lognormal realizations for the second redshift slice, compared to the adopted multivariate Gaussian model for the covariance. The full distribution does not contain significant wings that might cause confidence regions to be underestimated in subsequent cosmological parameter fits.
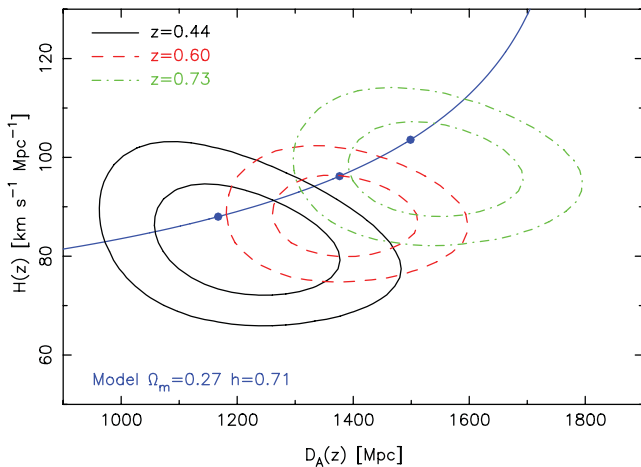

Figure 5. The joint likelihood of fits of $D_A(z)$ and $H(z)$ to the baryon acoustic peak and AP distortions in each of three overlapping WiggleZ redshift slices. The two contour levels in each case enclose regions containing 68.27 and 95.45 per cent of the total likelihood. A flat ΛCDM model prediction for cosmological parameters $\Omega_m = 0.27$ and $h = 0.71$ is plotted as the solid line, with circles representing the effective redshifts of the three data slices.

$H(z)$ with z is consistent with accelerating expansion given that $dH/dt = -H^2 [1 + (\ddot{a}/a)]$ is negative when $\ddot{a} > 0$. These measurements of $D_A(z)$ and $H(z)$ are listed in Table 1 along with the marginalized measurements of the normalized growth rate. The fractional accuracies with which the parameters are measured are 7–9 per cent for D_A and H, and 16–20 per cent for $f\sigma_8$. We note that readers wishing to include our data set in cosmological parameter fits should use the raw measurements of $(A, F, f\sigma_8)$ given in Table 1, together with the covariance matrix listed in Table 2, rather than these derived values of D_A and H.

4 COSMOLOGICAL MODEL FITS

We now use our joint WiggleZ measurements of the baryon acoustic peak and AP distortions to place constraints on parametric and non-parametric cosmological models, both alone and in combination with other data sets.

4.1 Other cosmological data sets

Together with the new WiggleZ results described in this study, we add BAO distance measurements obtained from the 6-degree Field

Galaxy Survey (6dFGS; Beutler et al. 2011) and by applying 're-construction' to the sample of Sloan Digital Sky Survey (SDSS) luminous red galaxies (Padmanabhan et al. 2012). We also include the joint BAO and AP measurements recently reported by the Baryon Oscillation Spectroscopic Survey (BOSS; Reid et al. 2012).

We additionally use the 'Union 2' compilation of supernovae data by Amanullah et al. (2010), as obtained from the website http://supernova.lbl.gov/Union. This compilation of 557 supernovae includes data from Hamuy et al. (1996), Riess et al. (1999, 2007), Astier et al. (2006), Jha et al. (2006), Wood-Vasey et al. (2007), Holtzman et al. (2008), Hicken et al. (2009) and Kessler et al. (2009). When fitting cosmological models to this SNe data set we used the full covariance matrix of these measurements including systematic errors, as reported by Amanullah et al. (2010). We also performed an analytic marginalization over the unknown absolute normalization (Goliath et al. 2001; Bridle et al. 2002).

Finally, in some fits we include CMB data using the *Wilkinson Microwave Anisotropy Probe* (*WMAP*) 'distance priors' (Komatsu et al. 2009) using the 7-year *WMAP* results (Komatsu et al. 2011). The distance priors quantify the complete CMB likelihood via a three-parameter covariance matrix for the acoustic index ℓ_A, the shift parameter $\mathcal{R}$ and the redshift of recombination z_*, as given in table 10 of Komatsu et al. (2011). When deriving these quantities we assumed a physical baryon density $\Omega_b h^2 = 0.0226$, a CMB temperature $T_{CMB} = 2.725$ K and a number of relativistic degrees of freedom $N_{eff} = 3.04$.

4.2 *w*CDM fits to WiggleZ measurements

As an initial analysis we fitted a flat wCDM cosmological model to these data sets in which spatial curvature is fixed at $\Omega_k = 0$ but the equation-of-state w of dark energy is varied as a free parameter. We fitted for the three parameters $(\Omega_m, \Omega_m h^2, w)$ using flat, wide priors which extend well beyond the regions of high likelihood and have no effect on the cosmological fits. We only use the joint WiggleZ measurements of $A(z)$ and $F(z)$ in these fits, not the growth rate data. The extra complexity in the normalization of the clustering pattern required to fit $f\sigma_8(z)$ is analysed by Parkinson et al. (in preparation).

Fig. 6 displays the joint likelihood of the parameters (Ω_m, w) marginalizing over $\Omega_m h^2$, comparing the effects of adding different data sets to the *WMAP* distance priors. The combination with the joint WiggleZ measurements of $A(z)$ and $F(z)$ is illustrated by the (black) solid contours, with the (red) dashed contours showing the improvement compared to only using the WiggleZ measurements of $A(z)$. The results are consistent with, albeit with a significantly lower
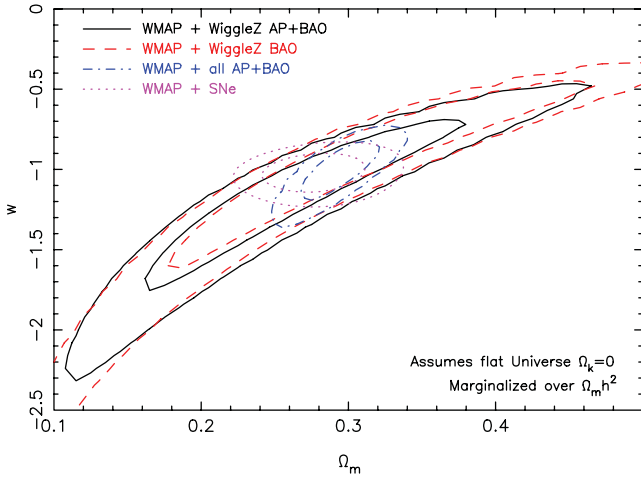
Figure 6. The joint probability for parameters Ω_m and w fitted to different data sets added to the *WMAP* distance priors, marginalizing over $\Omega_m h^2$ and assuming $\Omega_k = 0$. The CMB data are combined in turn with the WiggleZ acoustic scale and AP distortion measurements (with appropriate covariance; black solid contours), the WiggleZ acoustic scale measurements alone (red dashed contours), all BAO measurements (blue dash–dotted contours) and SNe distance data (magenta dotted contours). The two contour levels in each case enclose regions containing 68.27 and 95.45 per cent of the total likelihood.

accuracy than, parameter measurements based on the combination of the *WMAP* distance priors with all WiggleZ+BOSS AP+BAO data, and all SNe data, which are represented by the (blue) dash–dotted contours and (magenta) dotted contours, respectively.

4.3 $H(z)$ fits in bins

We performed a model-independent determination of the cosmic expansion history by carrying out a Monte Carlo Markov Chain (MCMC) fit for the Hubble parameter $H(z)$ as a stepwise function in narrow redshift bins, where we identify the value in the first bin as $H(z_1) = H_0 = 100\,h\,\mathrm{km\,s^{-1}\,Mpc^{-1}}$. We also included the spatial curvature Ω_k as a free parameter in our fit, such that we derived the angular diameter distance $D_A(z)$ from the comoving

radial coordinate $r(z)$ as

$$D_A(z) = r(z)/(1+z), \qquad \Omega_k = 0,$$
$$D_A(z) = R_{\mathrm{curv}} \sinh\left(r(z)/R_{\mathrm{curv}}\right)/(1+z), \qquad \Omega_k > 0,$$
$$D_A(z) = R_{\mathrm{curv}} \sin\left(r(z)/R_{\mathrm{curv}}\right)/(1+z), \qquad \Omega_k < 0, \qquad (2)$$

where $R_{\mathrm{curv}} = c/(H_0\sqrt{|\Omega_k|})$. If the range of the ith redshift bin is $z_{i,\min} < z < z_{i,\max}$, and the redshift at which we are evaluating a distance lies in the nth bin, the comoving radial coordinate $r(z)$ is deduced from the stepwise $H(z)$ function as

$$r(z) = \int_0^z \frac{c}{H(z')}\,\mathrm{d}z'$$
$$= \sum_{i=1}^{n-1} \frac{c\,(z_{i,\max} - z_{i,\min})}{H(z_i)} + \frac{c\,(z - z_{n,\min})}{H(z_n)}. \qquad (3)$$

Expressing this relation as a linear interpolation rather than a stepwise function makes little difference to the results. The availability of the WiggleZ and BOSS AP distortion measurements, with their direct sensitivity to $H(z)$, brings two significant benefits to this analysis: a more precise determination of $H(z)$ in stepwise bins, and a lower covariance between the measurements in different bins.

The left-hand panel of Fig. 7 illustrates the measurements of $H(z)$ in $N = 9$ stepwise redshift bins of width $\Delta z = 0.1$, where the likelihood is computed using the WiggleZ and BOSS joint BAO and AP data sets, the other BAO measurements from 6dFGS and SDSS and the SNe Union 2 data set. We note that we do not use the *WMAP* distance priors in this fit because of the uncertainty in extrapolating the expansion rate beyond our bins, in the redshift range $z_{N,\max} < z < z_*$, in order to deduce the value of $D_A(z_*)$ which is required to evaluate the quantities ℓ_A and $\mathcal{R}$. However, we do marginalize over a *WMAP*-motivated Gaussian prior in $\Omega_m h^2$ with mean 0.1345 and width 0.0055. This prior is used when fitting to the BAO data set, both when using the acoustic parameter $A(z) \propto \sqrt{\Omega_m h^2}$ and when calibrating the sound horizon scale $r_s(z_d)$. In the latter case we assume a fiducial baryon density $\Omega_b h^2 = 0.0226$. We also marginalize over a wide uniform prior in spatial curvature $-1 < \Omega_k < 1$.

We obtain measurements of $H(z)$ with precision better than 7 per cent in most $\Delta z = 0.1$ redshift bins in the range $z < 0.8$ (we note that the improved accuracy in the $0.7 < z < 0.8$ bin compared to the adjacent bins is due to the presence of the WiggleZ AP data point at $z = 0.73$). As displayed in Fig. 7, our measurements are consistent
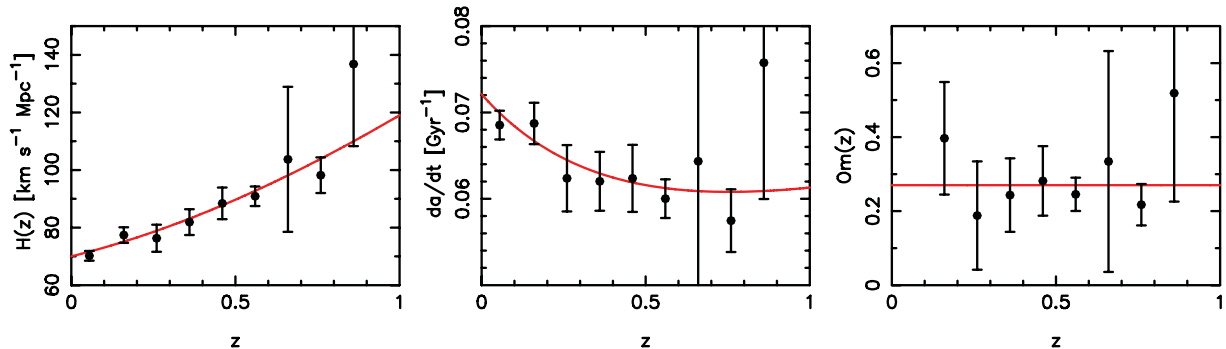

Figure 7. Panels displaying, from left to right, measurements of the Hubble parameter $H(z)$, the cosmic expansion rate $\dot{a} = H(z)/(1+z)$, and the 'Om' statistic $[[H(z)/H_0]^2 - 1]/[(1+z)^3 - 1]$ fit as a stepwise function in nine redshift bins of width $\Delta z = 0.1$ using a MCMC. The fit is performed to the WiggleZ and BOSS joint BAO and AP data sets, other BAO measurements from 6dFGS and SDSS, and SNe distance data. The measurement in each bin is marginalized over $H(z)$ in the other bins, the spatial curvature Ω_k and a *WMAP* prior for the sound horizon at baryon drag. The solid lines are not fits to the data but represent a fiducial flat ΛCDM cosmological model with parameters $\Omega_m = 0.27$ and $h = 0.71$. We do not plot a value for Om(z) in the first redshift bin because the statistic is not well defined in the limit $z \to 0$.
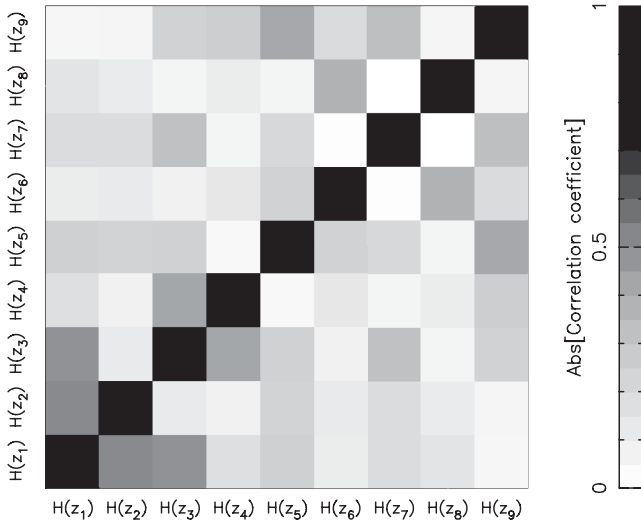
Figure 8. The matrix of correlation coefficients for the measurements of the Hubble parameter $H(z)$ in nine redshift bins plotted in Fig. 7, obtained using a MCMC.
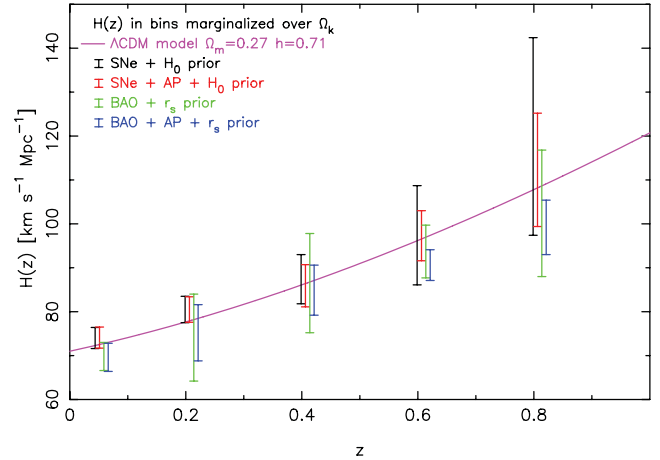

Figure 9. Measurements of the Hubble parameter $H(z)$ fit as a stepwise function in five redshift bins of width $\Delta z = 0.2$ using a MCMC. Results are compared for data sets SNe + H_0 prior, SNe + AP + H_0 prior, BAO + $r_s(z_d)$ prior and BAO + AP + $r_s(z_d)$ prior. The measurement in each bin is marginalized over $H(z)$ in the other bins and the spatial curvature Ω_k. The solid line is not a fit to the data but represents a fiducial flat ΛCDM cosmological model with parameters $\Omega_m = 0.27$ and $h = 0.71$.

Table 3. Measurements of the Hubble parameter $H(z)$, cosmic expansion rate $\dot{a} = H(z)/(1 + z)$ and 'Om' statistic $[[H(z)/H_0]^2 - 1]/[(1 + z)^3 - 1]$ fit as a stepwise function in nine redshift bins of width $\Delta z = 0.1$ using a MCMC. The fit is performed to the WiggleZ and BOSS joint BAO and AP data sets, other BAO measurements from 6dFGS and SDSS-DR7 and SNe distance data. The measurement in each bin is marginalized over $H(z)$ in the other bins, the spatial curvature Ω_k and a *WMAP* prior for the sound horizon at baryon drag. We do not quote a value for Om(z) in the first redshift bin because the statistic is not well defined in the limit $z \to 0$.

z	$H(z)$ (km s^{-1} Mpc^{-1})	$\dot{a}(z)$ (Gyr^{-1})	Om(z)
0.05	70.2 ± 1.7	0.0685 ± 0.0017	–
0.15	77.4 ± 2.7	0.0687 ± 0.0024	0.34 ± 0.15
0.25	76.3 ± 4.7	0.0624 ± 0.0038	0.15 ± 0.14
0.35	81.9 ± 4.5	0.0620 ± 0.0034	0.22 ± 0.10
0.45	88.4 ± 5.5	0.0624 ± 0.0039	0.26 ± 0.09
0.55	90.9 ± 3.4	0.0600 ± 0.0022	0.23 ± 0.04
0.65	103.7 ± 25.2	0.0643 ± 0.0156	0.32 ± 0.29
0.75	98.2 ± 6.2	0.0575 ± 0.0036	0.21 ± 0.05
0.85	136.8 ± 28.5	0.0758 ± 0.0158	0.50 ± 0.28

with a flat ΛCDM cosmological model with parameters $\Omega_m = 0.27$ and $h = 0.71$ (the value of the chi-squared statistic calculated using the full covariance matrix is 7.52 for 9 degrees of freedom). Fig. 8 displays the covariance between the measurements of $H(z)$ in each bin, deduced from the MCMC. The correlation coefficients between different bins vary depending on whether AP data are available, but are generally low or moderate, $r < 0.5$.

Table 3 lists the marginalized measurements of $H(z)$ in each bin. We also convert these measurements to values of the cosmic expansion rate $\dot{a} = \mathrm{d}a/\mathrm{d}t$ in physical units, where $a = 1/(1 + z)$ is the cosmic scale factor, and values of the 'Om' statistic (Sahni, Shafieloo & Starobinsky 2008) which is defined by

$$\mathrm{Om}(z) \equiv \frac{[H(z)/H_0]^2 - 1}{(1 + z)^3 - 1}. \qquad (4)$$

In a spatially flat ΛCDM model this statistic is constant at different redshifts and equal to today's value of the matter density

parameter Ω_m. In universes with different curvature, or containing dark energy with different properties to a cosmological constant, Om(z) would evolve with redshift. These determinations of $\dot{a}$ and Om(z) are plotted as the central and right-hand panels in Fig. 7, respectively. We see a significant decrease in the value of $\dot{a}$ between redshifts $z = 0$ and 0.7, corresponding to accelerating cosmic expansion. For example, the low-redshift expansion rate $\dot{a} = 0.069 \pm 0.002\,\mathrm{Gyr}^{-1}$ has dropped to $\dot{a} = 0.060 \pm 0.002\,\mathrm{Gyr}^{-1}$ at $z = 0.55$ and $\dot{a} = 0.058 \pm 0.004$ at $z = 0.75$. The measurements of Om(z) are consistent with a constant ≈ 0.25, as expected in a spatially flat ΛCDM model.

In Fig. 9 we compare the results of fitting $H(z)$ in five bins of width $\Delta z = 0.2$ to different subsets of the total data set. We note that, when combined with a CMB prior, the baryon oscillation scale is calibrated in units of Mpc and permits direct measurement of $H(z)$ in units of km s^{-1} Mpc^{-1}. However, given that the normalization of the supernova Hubble diagram is treated as an unknown parameter, the SNe data yield the relative luminosity distance $D_L(z)H_0/c$ and require an extra prior in H_0 in order to determine the function $H(z)$. We take this prior as the Riess et al. (2011) 3 per cent determination of the Hubble constant using new observations of Cepheid variables combined with Type Ia supernovae and the megamaser host galaxy NGC 4258, which yields a Gaussian prior in H_0 of mean 73.8 km s^{-1} Mpc^{-1} and standard deviation 2.4 km s^{-1} Mpc^{-1}. Fig. 9 illustrates the factor of 2–3 gain in precision at higher redshifts achieved when adding the WiggleZ and BOSS AP measurements, with their direct dependence on $H(z)$, to the existing BAO and SNe data set. It is also notable that the different probes produce consistent determinations of the expansion history within the statistical errors, which are consistent with a flat ΛCDM cosmological model with parameters $\Omega_m = 0.27$ and $h = 0.71$.

Another benefit of using the AP data set is a reduced covariance between the $H(z)$ measurements in different bins, which are heavily correlated when only total distance information is available. This is illustrated by Fig. 10, which displays the covariance between the $H(z)$ measurements in five bins for the case of SNe data + H_0 prior, illustrating the significantly higher correlation coefficients $r > 0.5$ in comparison with Fig. 8.
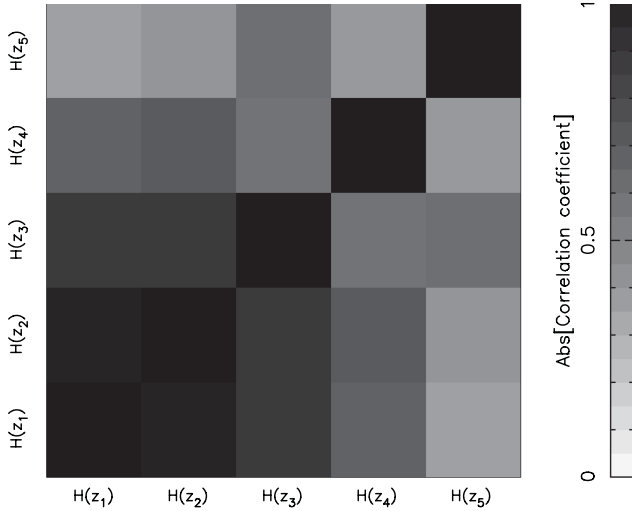
Figure 10. The matrix of correlation coefficients for the measurements of the Hubble parameter $H(z)$ in five redshift bins using just the SNe data set and H_0 prior, obtained using a MCMC.

Figure 11. The joint probability of kinematical model parameters q_0 and j fitted to different combinations of data sets and assuming $\Omega_k = 0$. Results are shown for SNe data alone, the BAO + AP data set and BAO + *WMAP*. The two contour levels in each case enclose regions containing 68.27 and 95.45 per cent of the total likelihood.

In order to illustrate further the consistent results obtained when varying the input data sets we fitted each determination of $H(z)$ plotted in Fig. 9 for the normalization factor h, assuming $\Omega_m = 0.27$, using the corresponding covariance matrix obtained from the Markov chain. The resulting measurements for the cases (SNe, SNe+AP, BAO, BAO+AP) were $h = (0.72 \pm 0.03, 0.72 \pm 0.03, 0.69 \pm 0.02, 0.68 \pm 0.02)$, respectively. (We note that the aim here is not to measure h, but to demonstrate that analysing these subsets of the data produces consistent results.)

4.4 Kinematical model fits

Finally, we fitted our data set with a 'kinematical' cosmological model (Rapetti et al. 2007) which is parametrized in terms of the dimensionless second and third derivatives of the scale factor $a(t)$ with respect to time, the deceleration parameter $q(t) = -H^{-2}(\ddot{a}/a)$ and jerk parameter $j(t) = H^{-3}(\dddot{a}/a)$. In particular, we adopt a parametrization where models are expressed in terms of the present-day value of the deceleration parameter q_0 and a constant jerk j, noting that ΛCDM models correspond to the special case $j = 1$. Following Rapetti et al. (2007), for a given (q_0, j) we determine the function

$$V(a) = -\frac{\sqrt{a}}{2}\left[\left(\frac{p-u}{2p}\right)a^p + \left(\frac{p+u}{2p}\right)a^{-p}\right], \quad (5)$$

where $p = \frac{1}{2}\sqrt{1 + 8j}$ and $u = 2(q_0 + \frac{1}{4})$. Given the function $V(a)$ we can determine the expansion rate as

$$\left[\frac{H(z)}{H_0}\right]^2 = -\frac{2\,V(a)}{a^2}. \quad (6)$$

We note that there is a region in the (q_0, j) plane defined by

$$j < q_0 + 2q_0^2, \quad q_0 < -1/4,$$
$$j < -1/8, \quad q_0 > -1/4 \quad (7)$$

for which the condition $V(a) \geq 0$ is not satisfied for all a and hence there is no big bang in the past. We exclude this region from our fits.

Fig. 11 illustrates the joint likelihood of kinematical model fits to the BAO, AP and SNe data sets. As in previous sections, we
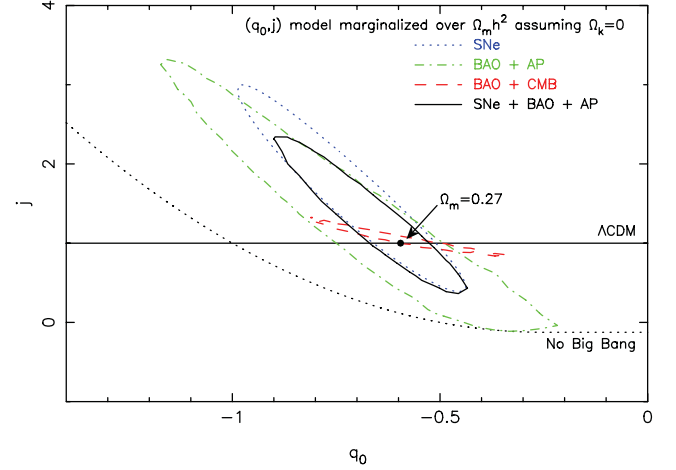
marginalize over a *WMAP*-inspired Gaussian prior in $\Omega_m h^2$ in order to calibrate the baryon oscillation standard ruler. ΛCDM models correspond to the line $j = 1$, and specific values of Ω_m pick out a point with $q_0 = \frac{3}{2}\Omega_m - 1$. These models are consistent with the data. We note that SNe provide the best constraints on the kinematical model parameters, and that including the *WMAP* distance priors in the fitted data set produces a very accurate joint constraint on (q_0, j) from the precisely known distance to the last-scattering surface, although this corresponds to a significant extrapolation of the validity of the model from $a > 0.5$ to >0.001. Fitting to the combination of SNe, BAO and AP data, not including the CMB, produces marginalized parameter measurements $q_0 = -0.67 \pm 0.16$ and $j = 1.37 \pm 0.68$.

5 CONCLUSIONS

We have used large-scale structure measurements from the WiggleZ Dark Energy Survey to perform joint fits for the baryon oscillation distance scale quantified by the acoustic parameter $A(z) \propto [D_A(z)^2/H(z)]^{1/3}$, the AP distortion parameter $F(z) \propto D_A(z)H(z)$ and the normalized growth rate $f\,\sigma_8(z)$ in three overlapping redshift slices with effective redshifts $z = (0.44, 0.6, 0.73)$. We use log-normal realizations to quantify the covariances between parameters and redshift slices, producing a 9×9 covariance matrix.

By combining the joint measurements of $A(z)$ and $F(z)$ taking into account the covariance, we performed simultaneous determinations of the angular diameter distance $D_A(z)$ and Hubble parameter $H(z)$ based only on the WiggleZ Survey data set and a *WMAP* prior in the matter density $\Omega_m h^2$ to calibrate the baryon oscillation standard ruler. These results are generally insensitive to the fiducial cosmological model including spatial curvature. We measure these parameters with 7–9 per cent accuracy in each redshift bin.

We use a combined data set consisting of these joint WiggleZ geometric measurements, other BAO data and SNe luminosity distances to perform a MCMC determination of the expansion history $H(z)$ as a stepwise function in nine redshift bins of width $\Delta z = 0.1$, also marginalizing over spatial curvature Ω_k. The results are consistent with a flat ΛCDM cosmological model with parameters

$\Omega_m = 0.27$ and $h = 0.71$. The addition of the AP data reduces both the errors in these measurements [through its direct sensitivity to $H(z)$] and the covariance between different redshift bins. When we convert our results to a measurement of the cosmic expansion rate $\dot{a} = H(z)/(1+z)$, we see a significant decrease in the value of $\dot{a}$ between redshifts $z = 0$ and 0.7, corresponding to accelerating cosmic expansion. Measurements of the statistic $Om(z) = [[H(z)/H_0]^2 - 1]/[(1+z)^3 - 1]$ are constant with redshift, consistent with a spatially flat ΛCDM model with matter density parameter $\Omega_m \approx 0.25$.

We compare our measurements to cosmological models including different dark energy equations-of-state w and kinematical models expressed in terms of the derivatives of the cosmic scale factor, the deceleration and jerk parameters. We find all data to be consistent with a cosmological constant model.

REFERENCES

Alcock C., Paczynski B., 1979, Nat, 281, 358
Amanullah R. et al., 2010, ApJ, 716, 712
Anderson L. et al., 2012, submitted (arXiv:1203.6594)
Astier P. et al., 2006, A&A, 447, 31
Ballinger W. E., Peacock J. A., Heavens A. F., 1996, MNRAS, 282, 877
Beutler F. et al., 2011, MNRAS, 416, 3017
Blake C. A., Glazebrook K., 2003, ApJ, 594, 665
Blake C. A. et al., 2011a, MNRAS, 415, 2876
Blake C. A. et al., 2011b, MNRAS, 418, 1707
Blake C. A. et al., 2011c, MNRAS, 418, 1725
Bridle S. L., Crittenden R., Melchiorri A., Hobson M. P., Kneissl R., Lasenby A. N., 2002, MNRAS, 335, 1193
Carson D. P., Nichol R. C., 2010, MNRAS, 408, 213
Conley A. et al., 2011, ApJS, 192, 1
Drinkwater M. et al., 2010, MNRAS, 401, 1429
Eisenstein D. J. et al., 2005, ApJ, 633, 560
Goliath M., Amanullah R., Astier P., Goobar A., Pain R., 2001, A&A, 380, 6
Hamuy M. et al., 1996, AJ, 112, 2408
Hicken M. et al., 2009, ApJ, 700, 331
Holtzman J. A. et al., 2008, AJ, 136, 2306
Jha S. et al., 2006, AJ, 131, 527
Jimenez R., Loeb A., 2002, ApJ, 573, 37
Kessler R. et al., 2009, ApJS, 185, 32
Komatsu E. et al., 2009, ApJS, 180, 330
Komatsu E. et al., 2011, ApJS, 192, 18
Marinoni C., Buzzi A., 2010, Nat, 468, 539
Matsubara T., Suto Y., 1996, ApJ, 470, 1
Moresco M. et al., 2012, submitted (arXiv:1201.3609)
Outram P. J., Shanks T., Boyle B. J., Croom S. M., Hoyle F., Loaring N. S., Miller L., Smith R. J., 2004, MNRAS, 348, 745
Padmanabhan N., White M., 2008, Phys. Rev. D, 77, 3540
Padmanabhan N. et al., 2012, submitted (arXiv:1202.0090)
Percival W. J. et al., 2010, MNRAS, 401, 2148
Perlmutter S. et al., 1999, ApJ, 517, 565
Rapetti D., Allen S. W., Amin M. A., Blandford R. D., 2007, MNRAS, 375, 1510
Reid B. A. et al., 2012, submitted (arXiv:1203.6641)
Riess A. G. et al., 1998, AJ, 116, 1009
Riess A. G. et al., 1999, AJ, 117, 707
Riess A. G. et al., 2007, ApJ, 659, 98
Riess A. G. et al., 2011, ApJ, 730, 119
Sahni V., Shafieloo A., Starobinsky A. A., 2008, Phys. Rev. D, 78, 3502
Seo H.-J., Eisenstein D. J., 2003, ApJ, 598, 720
Shafieloo A., Clarkson C., 2010, Phys. Rev. D, 81, 3537
Simpson F., Peacock J. A., 2010, Phys. Rev. D, 81, 3512
Sollerman J. et al., 2009, ApJ, 703, 2
Stern D., Jimenez R., Verde L., Kamionkowski M., Stanford A. S., 2010, J. Cosmol. Astropart. Phys., 2, 8
Suzuki N. et al., 2012, ApJ, 746, 85
Wang Y., Tegmark M., 2005, Phys. Rev. D, 71, 3513
Wood-Vasey W. M. et al., 2007, ApJ, 666, 694

This paper has been typeset from a TEX/LATEX file prepared by the author.